

Investigation of Magneto-Inductive Sensors for Low Magnetic Field Measurements

Huan Liu, *Member, IEEE*, Changfeng Zhao, Hongpeng Wang, Xiaobin Wang, Haobin Dong, Zheng Liu, *Senior Member, IEEE*, Jian Ge, Zhiwen Yuan, Jun Zhu, and Xinqun Luan

Abstract—The surface resistance reduction can further suppress the surface power loss of a superconducting radio-frequency cavity. Since the surface resistance of a superconducting radio-frequency cavity is mainly originated from the magnetic flux trapping, and thus the corresponding magnetic field strength could be measured to reflect the residual resistance. A fluxgate magnetometer is always employed to measure the ambient surface magnetic field of a superconducting radio-frequency cavity. However, this kind of equipment is relatively larger than the cavity and always need expensive cost. In this paper, we developed a magneto-inductive (MI) magnetic sensor, which is smaller, lighter weight, and lower cost than the fluxgate magnetometer. The specifications such as the noise floor, resolution, etc., are measured. In addition, a comparative observation of the magnetic field between the proposed MI sensor and a highly precise is conducted. The experimental results identify the capability of the proposed MI sensor in weak magnetic detection.

Index Terms—Magnetic field, magneto-inductive sensor, superconducting radio-frequency cavity.

I. INTRODUCTION

To achieve a High-Q operation of the superconducting radio-frequency cavity, numerous researches have been implemented [1], [2]. To be specific, since the cryogenic loss is tightly coupled to the High-Q operation, it is necessary to reduce the surface resistance of the superconducting radio-frequency cavity which is mainly originated from the magnetic flux trapping within the period of the cavity cooling down procedure [3], [4]. As the cavity cools down to a superconducting condition, the partial ambient magnetic field should be trapped into the radio-frequency cavity. In this case, we can obtain the surface residual resistance variations though measuring the corresponding magnetic field strength [5], [6].

This work is partly supported by the National Natural Science Foundation of China under Grant Nos. 41904164 and 41874212, the Foundation of Wuhan Science and Technology Bureau under Grant No. 2019010701011411 and 2017010201010142, the Foundation of National Key Research and Development Program of China under Grant No. 2018YFC1503702, the Foundation of Science and Technology on Near-Surface Detection Laboratory under Grant Nos. 6142414180913, TCGZ2017A001, and 614241409041217, and the Fundamental Research Funds for the Central Universities, China University of Geosciences (Wuhan) under Grant No. CUG190628.

H. Liu, C. Zhao, H. Wang, X. Wang, H. Dong, and J. Ge are with School of Automation, China University of Geosciences, Wuhan, China, and Hubei Key Laboratory of Advanced Control and Intelligent Automation for Complex Systems, Wuhan, China (email: huan.liu@cug.edu.cn).

Z. Liu is with School of Engineering, Faculty of Applied Science, University of British Columbia Okanagan Campus, Kelowna, Canada (email: zheng.liu@ubc.ca).

Z. Yuan, J. Zhu and X. Luan are with Science and Technology on Near-Surface Detection Laboratory, Wuxi, China.

Generally, a fluxgate sensor is employed to measure the ambient surface magnetic field of a superconducting radio-frequency cavity with high precision. However, this approach is not available to achieve a higher spatial resolution since the fluxgate sensor's size is relatively large [7], [8]. For instance, a commonly used and accepted fluxgate sensor, dubbed Mag-03, which is developed by with dimensions of 32 mm x 32 mm x 225 mm [9], [10]. In recent years, a kind of magnetic sensor using magneto-inductive (MI) technique has gradually entered the field of weak magnetic detection [11], [12]. The measurement principle of the MI sensor is conspicuously different from that of the fluxgate sensor. Because of its miniature size, the MI sensor has been commonly employed in many applications, such as compassing, inertial navigation, security system, etc [13]–[15].

In this paper, we develop a MI sensor to measure the surface magnetic field of the superconducting radio-frequency cavity. The electrical properties including the noise floor, resolution, magnetic tracking performance, etc., are evaluated in the Laboratory of Advanced Magnetic Sensor and Intelligent Imaging Detection, China University of Geosciences, Wuhan, China. Moreover, a measurement system using the MI sensor is developed to conduct an outdoor contrast experiment with a commercial Overhauser magnetometer and its performance for magnetic anomaly detection is verified.

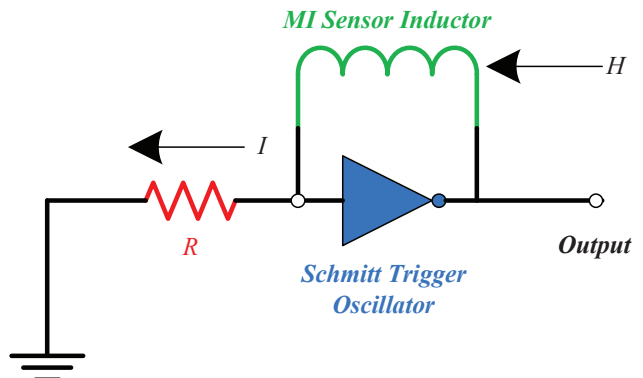


Fig. 1: Diagram of the electrical components involved in the magneto-inductive technique.

II. MAGNETO-INDUCTIVE SENSOR

The MI sensor mainly consists of a resistor-inductor circuit, in which an electronic component is sensitive to the external magnetic field. To be specific, as shown in Fig. 1,

the period during the charging and discharging procedures of the MI sensor inductor between two thresholds (lower and upper) through the Schmitt trigger oscillator, is proportional to the external magnetic field strength H . Generally, the total magnetic field H_t is composed of the external magnetic field H and the generated field kI of the circuit as:

$$H_t = H + kI \quad (1)$$

where k stands for the conversion factor of the sensor coil, and I stands for the generated current. In this case, the Schmitt trigger would operate the I through the resistor R to oscillate since the generated voltage of R is over than the setting trigger value. More details about the operation principle of the MI sensor can be referred to literature [16].

A MI sensor module is constructed as shown in Fig. 2, which consists of one sensor coil (PN 13101) for z axis, two sensor coils (PN 13104) for x and y axis, respectively. Further, an application-specific integrated circuit controller is embedded in this module, which can transfer the analog data to a digital format. In this case, we can obtain the external magnetic field value through deriving the digital data to a micro-controller directly, which can avoid the additional signal conditioning module and acquisition module as that in a fluxgate sensor.

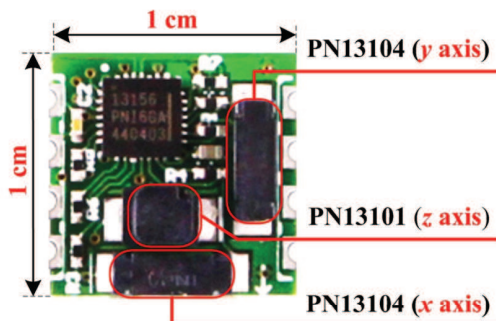


Fig. 2: Three-axis MI hybrid sensor.

III. EXPERIMENTAL RESULTS AND DISCUSSION

In this section, the specifications of the proposed MI sensor including the resolution, the noise floor, the stability, and the magnetic tracking performance are evaluated by using a magnetic shielding cylinder with three layers, which can further suppress the external magnetic field and electro magnetic interference. In this case, the measurement range of the MI sensor is set as $-800 \mu\text{T}$ to $800 \mu\text{T}$, the digital resolution is 13.33 nT per least significant bit, and the sampling rate is 10 Hz.

A. Platform setup

We set up a magnetic field measurement system using the proposed MI sensor as illustrated in Fig. 3, this system mainly consists of four modules, i.e., a MI sensor, a micro-controller, a USB serial controller, and an upper computer. Hence, the magnetic field data collected by the MI sensor can be transferred to the computer through the serial port,

and ultimately achieve real-time monitoring. Further, a least squares based data smoothing method is employed to suppress the fluctuations of the anomalous data, further improving the signal to noise ratio (SNR) of the measured data.

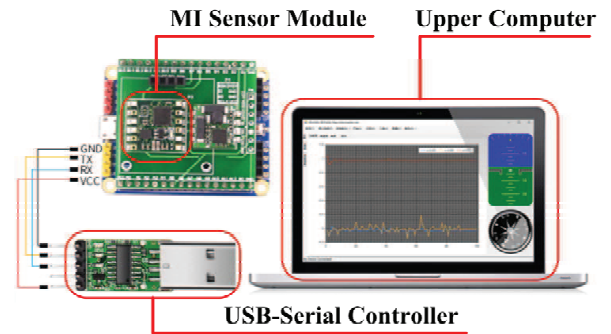


Fig. 3: Testing platform of the proposed MI magnetic field sensor system.

B. Resolution

Theoretically, the resolution stands for the minimum detection value of the MI sensor, and the standard deviation can be adopted to evaluate the resolution [17]. The standard deviation can be written as:

$$\delta = \sqrt{\frac{1}{n-1} \sum_{i=1}^n (y_i - \bar{y}_i)^2} \quad (2)$$

where δ stands for the standard deviation, \bar{y}_i stands for the average value, and n stands for the number of the collected data. Fig. 4 shows the collected continuous data within 10 minutes. Through Eq. 2, we can calculate the resolution as about 8.28 nT. This value is lower than the digital resolution we set as 13.33 nT, because we implement an averaging operation for every ten data to further improve the resolution. Ideally, the larger the number of averaging data, the better the resolution. However, this will influence the dynamical response characteristic of the MI sensor.

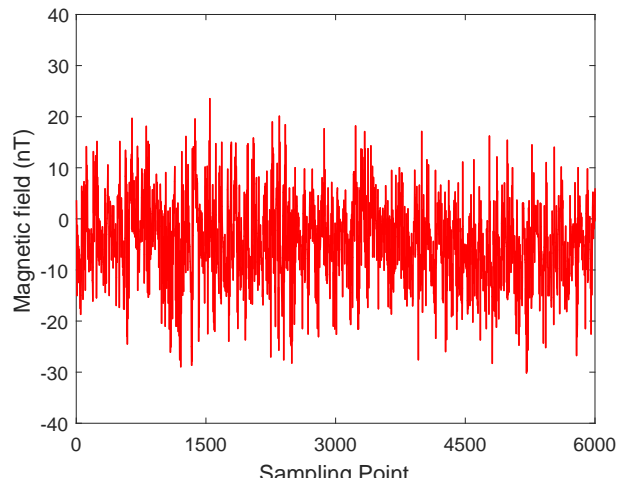


Fig. 4: Zero applied field measurement results.

C. Noise floor

Since the frequency characteristic of the noise features a $1/f$ dependence, the power spectral density at 1 Hz is always employed to evaluate the noise floor of a sensor [18], [19]. Hence, we collect the magnetic field data consecutively within 1 hour. Fig. 5 shows the evaluating results of the power spectral density. We can see that the noise floor of the $1/f$ region is relatively high, and it decreases slowly overall with up and down fluctuations as the frequency increases. As the frequency increases around 1 Hz, the total noise tends to be stable and the noise floor of the developed MI sensor is about $0.235 \text{ nT/Hz}^{1/2}$ at 1 Hz.

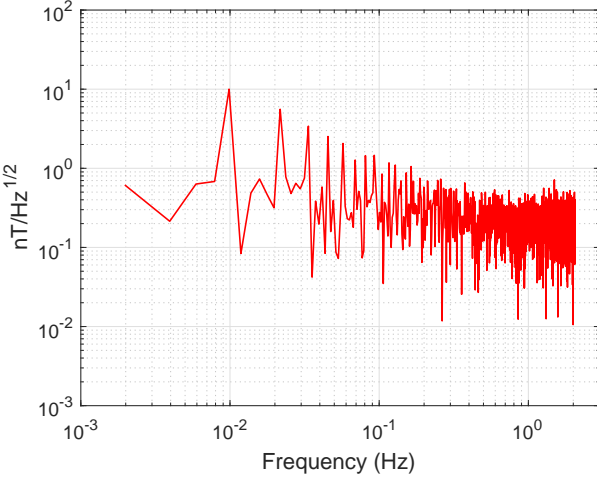


Fig. 5: Power spectral density of the proposed MI sensor module.

D. Stability

The stability of the sensor represents how constant the collected data is when there is no external magnetic field [20]. To evaluate the stability of the proposed MI sensor, the sensor is also placed in the magnetic shielding cylinder without an external magnetic field but might be accompanied by a little bit residual of the geomagnetic field. The system is operating for about 1 hour with a sampling rate of 10 Hz. Fig. 6 shows a histogram with the distribution of the collected data. It can be seen that the distribution is normal with an approximate symmetrical shape, and the value of the symmetrical center is about 0 nT. In addition, the randomness of the observed variations is corresponding to the intrinsic noise of the sensor.

E. Magnetic tracking performance

Further, we adopt the magnetic field shielding cylinder to generate a changeable magnetic field while the step values including 50 nT and 100 nT, to identify its magnetic tracking performance. The measurement results are shown in Fig. 7. We observe that the proposed MI-based magnetometer can track the variation of 100 nT effectively, while for the 50 nT the magnetic tracking performance is less satisfactory (with

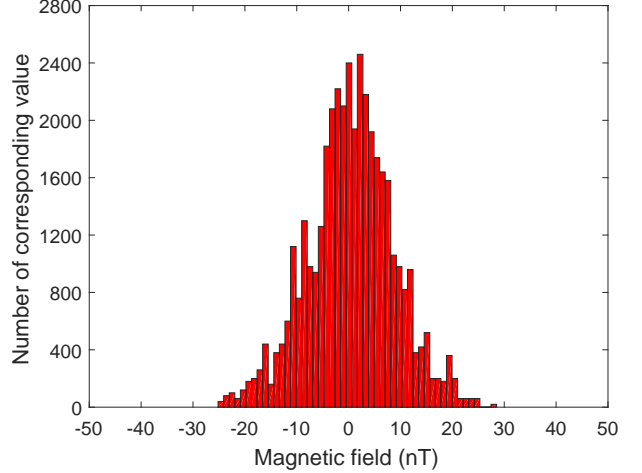


Fig. 6: Distribution of collected data within one hour.

major fluctuations) than that of 100 nT. In addition, there is one thing that needs to be emphasized. During the experiment, we observe that when the step value is lower than 50 nT, the magnetic tracking performance is not obvious due to the own noise properties of the MI sensor. Hence, we only depict the testing results of 100 nT and 50 nT in this paper.

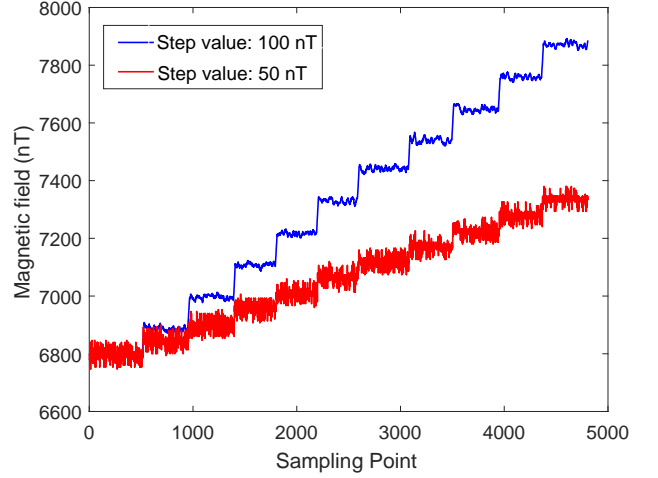


Fig. 7: The measurement results of the magnetic tracking performance.

F. Geomagnetic comparison test

To further identify the performance of the developed MI sensor system, a comparison testing between this sensor and a commercial Overhauser sensor system was implemented to observe the magnetic field during the same period. Moreover, we place a iron (the shape is cylinder and the dimension is about 80 mm x 80 mm x 200 mm) near the aforementioned two sensors with different distances (30 cm and 100 cm), to verify the capability for magnetic anomaly detection. The local magnetic field strength is about 49660 nT and the magnetic field measurement results are shown in Fig. 8.

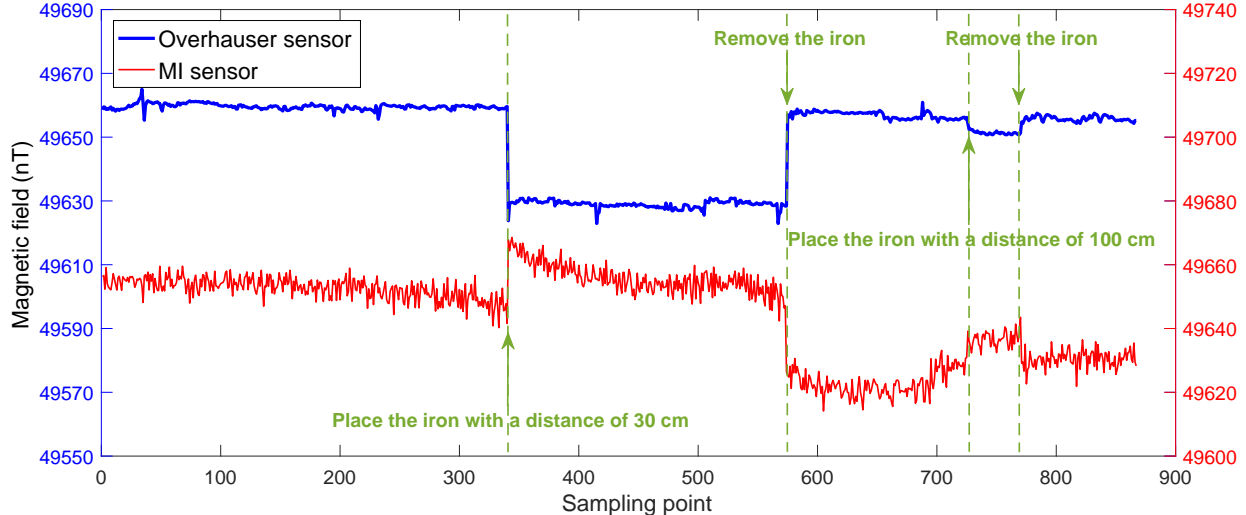


Fig. 8: Contrast test between the proposed MI sensor and the commercial Overhauser sensor.

Firstly, the trends of the geomagnetic field intensity measured by these two instruments are basically the same, while during the anomaly detection stage, the two recording curves are opposite and symmetric. The main reason is that in order to avoid magnetic interference, the two magnetometers are placed far away from each other (5 m in this paper), and the different sensor positions will generate a magnetic field gradient. Besides, since the iron is placed between the two sensors, there will generate two opposite magnetic anomalies at the head and the tail of the iron according to its magnetic field distribution characteristics [19]. Further, the fixed magnetic anomalies of buildings, vehicles, and cables in the test environment also generate magnetic field gradients, but they do not affect the contrast between the two sensors. Under the influence of moving pedestrians and vehicles in the test environment, the external magnetic interference cannot be completely avoided. The consistent variation trend of the commercial Overhauser sensor and the MI sensor indicates that our proposed MI sensor has good magnetic field tracking performance and is sensitive to the magnetic anomalies in the measured area.

IV. CONCLUSIONS

In this study, we developed a miniature MI sensor module with dimensions of 1 cm x 1cm x 0.2 cm to measure the surface magnetic field of the superconducting radio-frequency cavity. The laboratory testing results demonstrate that the proposed MI sensor can detect a low magnetic field strength as low as 8.28 nT when the sampling rate is 10 Hz, and its typical noise floor is about 0.235 nT/Hz^{1/2} at 1 Hz. For the field testing results, the proposed MI sensor shows good magnetic field tracking performance, and has the ability to catch magnetic anomalies. Consequently, the proposed MI sensor shows a great scope for magnetic anomaly detection, and the miniature property makes it overcome the shortcomings of the related commercial devices (especially the fluxgate sensor) for measuring the surface magnetic field of the superconducting radio-frequency cavity, i.e., bulky size, heavy, high power, etc.

Further, this study also lays the foundation for future works to improve the accuracy of the MI sensor for magnetic field detection.

REFERENCES

- [1] R. Ueki, T. Okada, M. Masuzawa, K. Tsuchiya, T. Kawamoto, K. Umemori, E. Kako, T. Konomi, and H. Sakai, "Study on magnetoresistance sensors for low magnetic field measurements," *IEEE Transactions on Applied Superconductivity*, vol. 30, no. 4, pp. 1–4, 2020.
- [2] K. Umemori, T. Dohmae, E. Kako, T. Konomi, T. Kubo, M. Masuzawa, T. Okada, G.-T. Park, A. Terashima, K. Tsuchiya *et al.*, "Improvement of magnetic condition for kek-srf vertical test facility toward high-q study," in *Proc. 18th Int. Conf. on RF Superconductivity (SRF'17)*, 2017, pp. 444–447.
- [3] A. Romanenko, A. Grassellino, A. Crawford, D. Sergatskov, and O. Melnychuk, "Ultra-high quality factors in superconducting niobium cavities in ambient magnetic fields up to 190 mg," *Applied Physics Letters*, vol. 105, no. 23, p. 234103, 2014.
- [4] M. Masuzawa, K. Tsuchiya, and A. Terashima, "Study of magnetic shielding materials and fabrication of magnetic shield for superconducting cavities," *IEEE Transactions on Applied Superconductivity*, vol. 24, no. 3, pp. 1–4, 2013.
- [5] K. Umemori, H. Hara, H. Inoue, E. Kako, T. Konomi, T. Kubo, H. Sakai, K. Sennyu, H. Shimizu, M. Yamanaka *et al.*, "Vertical test results of nitrogen doped srf cavities at kek," in *7th Int. Particle Accelerator Conf.(IPAC'16), Busan, Korea, May 8-13, 2016*. JACOW, Geneva, Switzerland, 2016, pp. 2154–2157.
- [6] H. Liu, H. Dong, J. Ge, Z. Liu, Z. Yuan, J. Zhu, and H. Zhang, "Apparatus and method for efficient sampling of critical parameters demonstrated by monitoring an Overhauser geomagnetic sensor," *Review of Scientific Instruments*, vol. 89, no. 12, p. 125109, 2018.
- [7] B. Bai, H. Liu, J. Ge, and H. Dong, "Research on an improved resonant cavity for overhauser geomagnetic sensor," *IEEE Sensors Journal*, vol. 18, no. 7, pp. 2713–2721, 2018.
- [8] H. Liu, H. Dong, J. Ge, Z. Liu, Z. Yuan, J. Zhu, and H. Zhang, "A fusion of principal component analysis and singular value decomposition based multivariate denoising algorithm for FID transversal data," *Review of Scientific Instruments*, vol. 90, no. 3, p. 035116, 2019.
- [9] B. Instruments, "Mag-03 three axis magnetic field sensors," 2014.
- [10] H. Liu, H. Dong, J. Ge, and Z. Zhao, "Magnetic field gradient detector based on the nuclear overhauser effect," *Chinese Journal of Scientific Instrument*, vol. 36, no. 3, pp. 592–600, 2015.
- [11] H. Liu, X. Wang, H. Wang, J. Bin, H. Dong, J. Ge, Z. Liu, Z. Yuan, J. Zhu, and X. Luan, "Magneto-inductive magnetic gradient tensor system for detection of ferromagnetic objects," *IEEE Magnetics Letters*, vol. 11, no. 1, p. 8101205, 2020.

- [12] M. Moldwin, B. Bronner, L. Regoli, J. Thoma, A. Shen, G. Jenkins, and J. Cutler, "New magneto-inductive dc magnetometer for space missions," in *AGU Fall Meeting Abstracts*, 2017.
- [13] H. Liu, H. Dong, Z. Liu, J. Ge, B. Bai, and C. Zhang, "Construction of an overhauser magnetic gradiometer and the applications in geomagnetic observation and ferromagnetic target localization," *Journal of Instrumentation*, vol. 12, no. 10, p. T10008, 2017.
- [14] Y. Huang, J. Ge, H. Dong, and H. Liu, "An automatic wideband 90° phase shifter for optically pumped cesium magnetometers," *IEEE Sensors Journal*, vol. 17, no. 23, pp. 7928–7934, 2017.
- [15] H. Liu, X. Wang, J. Bin, H. Dong, J. Ge, Z. Liu, Z. Yuan, J. Zhu, and X. Luan, "Magnetic gradient full-tensor fingerprints for metallic objects detection of a security system based on anisotropic magnetoresistance sensor arrays," *AIP Advances*, vol. 10, no. 1, p. 015329, 2020.
- [16] A. Leuzinger and A. Taylor, "Magneto-inductive technology overview," *PNI white paper*, 2010.
- [17] H. Dong, H. Liu, J. Ge, Z. Yuan, and Z. Zhao, "A high-precision frequency measurement algorithm for fid signal of proton magnetometer," *IEEE Transactions on Instrumentation and Measurement*, vol. 65, no. 4, pp. 898–904, 2016.
- [18] H. Liu, H. Dong, J. Ge, B. Bai, Z. Yuan, and Z. Zhao, "Research on a secondary tuning algorithm based on svd & stft for fid signal," *Measurement Science and Technology*, vol. 27, no. 10, p. 105006, 2016.
- [19] H. Liu, H. Dong, Z. Liu, J. Ge, B. Bai, and C. Zhang, "Noise characterization for the fid signal from proton precession magnetometer," *Journal of Instrumentation*, vol. 12, no. 7, p. P07019, 2017.
- [20] H. Liu, H. Dong, Z. Liu, J. Ge, W. Luo, C. Zhang, Z. Yuan, J. Zhu, and H. Zhang, "A comprehensive study on the weak magnetic sensor character of different geometries for proton precession magnetometer," *Journal of Instrumentation*, vol. 13, no. 09, p. T09003, 2018.